JP Journal of Heat and Mass Transfer
© 2016 Pushpa Publishing House, Allahabad, India
Published: November 2016
http://dx.doi.org/10.17654/HM013040511
Volume 13, Number 4, 2016, Pages 511-532 **ISSN: 0973-5763**

EFFECT OF RADIATOR TYPE ON DRYER ROOM TEMPERATURE DISTRIBUTION AND HEAT TRANSFER RATE

M. Mirmanto, E. D. Sulistyowati and I. K. D. Okariawan

Mechanical Department
Mataram University
Jl. Majapahit No. 62, Mataram
NTB, 83125, Indonesia
e-mail: mmirmanto@gmail.com

Abstract

Radiator types may affect the drying method or drying speed. Experiments to investigate the effect of a radiator type on a room temperature distribution and heat transfer rate were conducted. There were three radiator types used in this work, i.e., parallel radiator (Case A), finned radiator (Case B) and serpentine radiator (Case C). The prototype room with an overall size of $1000\text{mm} \times 1000\text{mm} \times 1000\text{mm}$ was made of plywood and employed in this study while the radiators were made from copper pipes and aluminium fins. The water temperature at the entrance was increased gradually at 0 to 1000s and then kept at 80°C. The maximum temperature of 50°C was reached in the prototype room and shown by the closest thermocouple to the radiator. In general, Case A is the best radiator type and recommended as a heat source in a dryer room.

Received: May 7, 2016; Accepted: July 2, 2016
Keywords and phrases: radiator, dryer room, temperature distribution, heat transfer rate.
Communicated by Lingen Chen

Nomenclature

A	: Heat transfer area (m^2)
C	: Constant for free convection Nusselt number determined in the experiment
c_p	: Specific heat (J/kg K)
D	: Diameter (m)
g	: Earth gravity $(\mathrm{m/s}^2)$
Gr	: Grashof number, $Gr = \frac{g\beta(T_{wo} - T_r)D_o^3}{\nu^2}$
h	: Heat transfer coefficient $(\mathrm{W/m^2K})$
H	: Fin width (m)
ID	: Inner diameter (m)
k	: Thermal conductivity (W/m K)
L	: The length of the test section (m)
m	: The power of the Nusselts number correlation determined in the experiment
$\dot{m}$	: Mass flow rate (kg/s)
n	: Number of fin
$\overline{Nu}$	: Nusselts number, $\overline{Nu} = hD/k$
OD	: Outer diameter (m)
PID	: Proportional-integral-derivative controller
q	: Heat transfer rate (W)
q_w	: Heat transfer rate of water (W)

q''	:	Heat flux $(\mathrm{W/m^2})$
r	:	Radius (m)
R	:	Thermal resistance (K/W)
Ra	:	Rayleigh number, $Ra = GrPr$
S	:	Fin spacing (m)
T	:	Temperature (°C)

Greek symbols

β	:	Expansion coefficient (1/K)
ν	:	Kinematic viscosity $(\mathrm{m^2/s})$
Δ	:	Delta

Subscript

b	:	Bulk
i	:	Inlet
f	:	Fluid
o	:	Outlet, outer
p	:	Pipe
r	:	Room
s	:	Fin
wi	:	Inner wall
wo	:	Outer wall

1. Introduction

In practice, the term “radiator” refers to any of a number of devices in which a fluid circulates through exposed pipes. Never mind that such devices tend to transfer heat mainly by convection. This is because the term convector refers to a class of devices in which the source of heat is not directly exposed. Therefore, in this study, the test section is called *radiator*.

A room radiator can be used for drying goods such as agricultural products, foods and clothes. This drying method is indeed useful particularly in the rainy season where the sun cannot shine due to much rains or clouds. However, when it is run using an electrical or fossil energy, the dried goods become more expensive due to the drying cost. Thus, a wise way to support this purpose should be invented. This wise way is just to utilize heat wastes, e.g., heat waste from food production or industrial processes, or from biomass, biogas and gasification, see Coronado et al. [1]. Nevertheless, this drying method has not been introduced until nowadays. For the reason, the authors are encouraged to perform a research on this subject and expect this subject useful for everybody who performs drying process for their goods. One of the difficulties of this study is the limited suitable literature due to no research on this drying method yet. Moreover, it is expected to improve the conventional radiator which usually has a big gap or needs much hot water.

Types of the radiator that are available in the market are corrugated plate, parallel pipe and finned radiator. Nevertheless, finned radiator is easy to get dirt and difficult to clean. Almost all radiators are run using hot water, hence one may call it *hot water radiator*. A hot water radiator consists of a sealed hollow metal container filled with hot water by gravity feed, a pressure pump, or convection. As it gives out heat, the hot water cools and sinks to the bottom of the radiator and is forced out of a pipe at the other end. Anti-hammer devices are often installed to prevent or minimize knocking in hot water radiator pipes. Traditional cast iron radiators are no longer common in new construction, replaced mostly with forced hot water baseboard style radiators. They consist of copper pipes which have aluminium fins to increase their surface area. These conduction boiler systems use conduction to transfer heat from the water into the metal radiators or convectors. The radiators are designed to heat the air in the room using convection to transfer heat from the radiators to the surrounding air. They do this by drawing cool air in at the bottom, warming the air as it passes over the radiator fins, and discharging the heated air at the top. This sets up convective loops of air movement within a room. If the register is blocked either from above or below, then this air movement is prevented, and the heater will not work. Baseboard heating systems are sometimes fitted with moveable covers to allow the resident to fine-tune heating by room, much like air registers in a central air system.

Mirmanto et al. [2] have been working in this subject to introduce a new drying method using a radiator where the heat source can be obtained from heat waste or biomass. Almost previous studies that focused on radiator researches, mostly explored water flow and ventilation for the radiator. Myhren and Holmberg [3] studied the performance of ventilation radiators that could be improved by changing the geometry of internal convection fins. Their data were used to validate the CFD investigation. Ploskic and Holmberg [4] evaluated radiant baseboard room heaters and validate a correlation of heat output that according to them the heat output could be estimated using an equation as given by

$$P = \dot{m}c_p(\theta_{supp} - \theta_{rtn}) = UA\Delta\theta_{LMTD}, \tag{1}$$

where P is the heat output (W), θ is the temperature (°C), $\Delta\theta$ refers to mean temperature difference between room heater and room air. U is the overall heat transfer coefficient, A is the heat transfer area and $\dot{m}$ is the mass flow rate. While Bangert [5] enhanced heat transfer from a radiator to the room by coating the wall behind the radiator. Embaye et al. [6] conducted a simulation investigation to improve the performance of a central radiator using pulsation mass flow rates. They elucidated that their method could save energy by up to 22%. Even it could reach 27% when the pulsation was controlled using a PID. Nevertheless, Embaye et al. [6] might not consider the pump power for “on and off”. The energy used by the pump may fluctuate due to the pulsation but at the starting time to run (on-off), the pump needs bigger energy. Thus, this also should be considered to operate the radiator using this method. Similar experiments using flow rate pulsations were also introduced by Lemlich [7], Shuai et al. [8] and Zohir [9], but they investigated heat transfer rates in heat exchangers.

On the other hand, some studies prefer to explore control strategies to improve its energy use and carbon emission. Liu et al. [10] applied a new technique to monitor and control the energy consumed by the heating system. Using their method, the claimed that they could reduce the energy consumed up to 30%. Lehmanna et al. [11] and Adolph et al. [12] also tried to reduce the use of the energy. The energy used for heating the room is not only depended on the heat transferred from the radiator to the room but also the amount of water flow rates. Increasing the mass flow rate raises the energy use for both pumping and heating. In contrast, the effect of mass flow rate on the heat transfer rate is not significant, see Calisir et al. [13] and Mirmanto et al. [14].

As explained in [14], conventional room radiators are usually constructed from thick iron or stainless steel materials. Due to the big gap, not all of the hot water molecules inside the radiator touch the radiator walls, consequently, the heat transfer rate is low and needs much energy for heating the water. In this study, the radiator is constructed from small/mini copper pipes with aluminium fins expected to increase/enhance the heat transfer performance, see Qu and Mudawar [15], Venkatesan et al. [16], Mirmanto [17] and Wang and Sefiane [18]. They explained that as the diameter of the channel decreased, the heat transfer coefficient increased. The slim radiator made of small copper pipes reduces the amount of hot water and consequently the pumping and heating power consumed. Nevertheless, none of those above literatures (except Mirmanto et al. [2]) expose a research on the use of radiator as the heat source of a room dryer.

From the above paragraphs, several motivations or objectives can be drawn as follows: (i) plenty of free energy in the nature such as heat waste, biomass, biogas, geothermal can be used to operate this drying method, (ii) this drying method needs to be introduced and implemented, (iii) to know the effect of radiator type on the room temperature distribution and heat transfer rate, (iv) to know the possible maximum room temperature, (v) to check the free heat transfer coefficient that is assumed of approximately $7\text{-}10\,\mathrm{W/m^2K}$ as used in Ploskic and Holmberg [4], Embaye et al. [6] and Qu and Mudawar [15].

2. Experimental Facilities and Set Up

The schematic diagram of the test rig, as shown in Figure 1, consisting of a main reservoir, a centrifugal pump, calibrated flow meter, three electrical heaters controlled using PIDs, a gas heater, radiators and a prototype room. The working fluid (water) was flowed and circulated through the entire test rig using the centrifugal pump shimizu while the secondary working fluid (air) was circulated naturally due to the temperature difference. In the four heaters, the water was heated up to the desired temperature. Leaving the heaters, the water then flowed to the radiator and released heat to the air inside the prototype room. A water mass flow rate of $12.5 \mathrm{g/s}$ was employed in the experiments and measured using a calibrated flow meter model FLR1012ST-D with an uncertainty of $\pm 0.5 \mathrm{g/s}$ obtained from the weighted calibration method using a digital balance and stop watch. The inlet temperature was increased gradually and then kept at 80°C at the radiator entrance.

The radiator was constructed from copper pipes arranged in several types, i.e., parallel radiator (Case A), finned pipe radiator (Case B) and serpentine radiator (Case C) as provided in Table 1. A prototype room with an overall dimension of $1000\mathrm{mm} \times 1000\mathrm{mm} \times 1000\mathrm{mm}$ was tested and constructed from a wood frame and plywood with a thickness of 5mm. The construction of the radiator is presented in Figure 2.

All temperatures were measured using calibrated T type thermocouples with an uncertainty of ±0.5°C. The data were continuously recorded every second until all temperatures inside the prototype room were steady or approximately for about 3500 seconds.

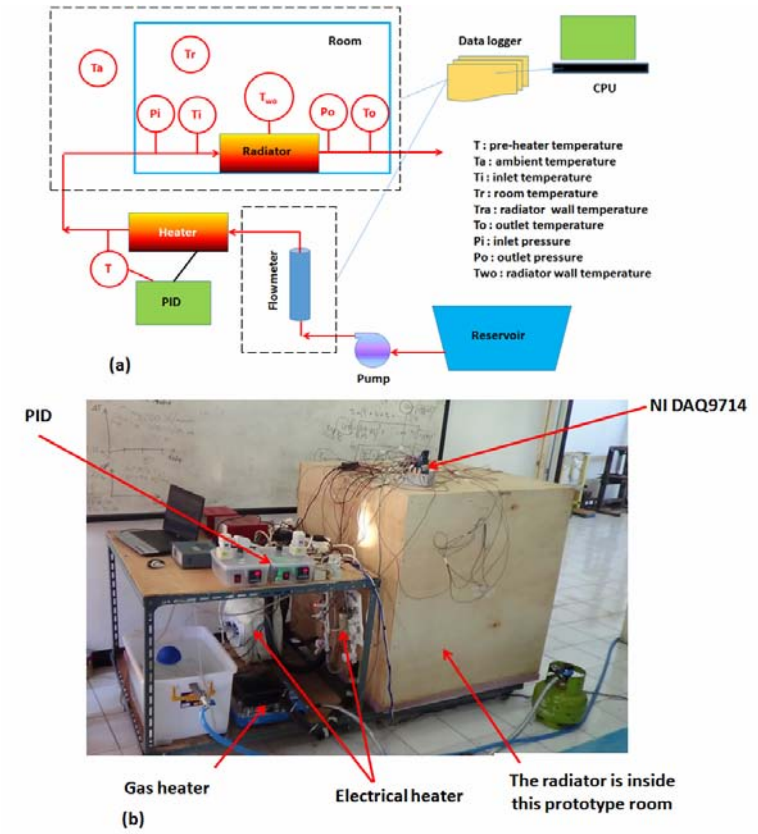

Figure 1. (a) Schematic diagram of the test rig and (b) photograph. All sensors are connected to the NI DAQ9714.

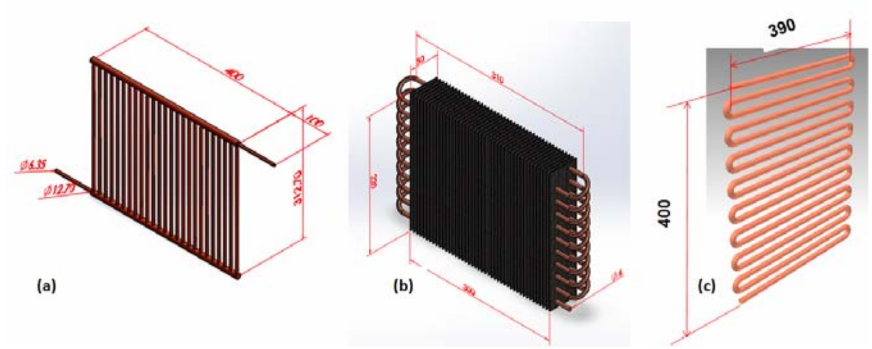

Figure 2. Radiator construction: (a) Case A, (b) Case B and (c) Case C.

Table 1. Dimension, radiator types and materials

Radiator type	Dimension	Material
Parallel pipe radiator (Case A)	Pipe dimension: 6.35mm OD, 4.45mm ID	Copper
	Overall: 6.35mm × 312.7mm × 400mm	
	Pipe number: 25	
	Header diameter OD: 12.7mm	
	Header diameter ID: 10.9mm	
	Total outer heat transfer area A_o: 0.185m^2	
Finned pipe radiator (Case B)	Fin dimension: 50mm wide, 220mm high	Fin: aluminium
	Pipe dimension: 6.35mm OD, 4.45mm ID	Pipe: copper
	Overall: 50mm × 220mm × 330mm	
	Fin number: 45	
	Fin spacing: 5mm	
	Pipe pass number: 20	
	Total outer heat transfer area A_o: 0.56m^2	
Serpentine radiator (Case C)	Pipe dimension: 6.35mm OD, 4.45mm ID	Copper
	Total pipe length: 7.02m	
	Pipe pass number: 18	
	Total outer heat transfer area A_o: 0.14m^2	

3. Data Reduction

There are two phenomena that are investigated experimentally in this present study, (1) heat transferring from hot water to the radiator wall and fins and (2) heat transferring from the radiator wall and fins to the air inside the prototype room. The heat transferred from hot water to the radiator wall and fins is predicted using a steady flow energy equation, as elucidated in

Holman [19] and Incropera et al. [20]:

$$q_w = \dot{m}c_p(T_i - T_o) \tag{2}$$

which is actually the same as equation (1), where q_w is the rate of heat transfer of the hot water, $\dot{m}$ represents the mass flow rate of hot water, T_i is the hot water inlet temperature and T_o is the hot water outlet temperature. Note that in this study, T_i is higher than T_o. c_p refers to the specific heat of hot water and is evaluated using the bulk hot water temperature. The heat transferring from the water to the air is estimated using an equation presented in Holman [19] and is given by:

$$q = \frac{T_b - T_r}{\frac{1}{h_i A_i} + \frac{\ln(r_o/r_i)}{2\pi k_p L_p} + \frac{1}{h_o A_o}}, \tag{3}$$

where T_b is the fluid (water) bulk temperature $(T_i + T_o)/2$, T_r is the average temperature of air inside the prototype room, h_i is the heat transfer coefficient of water inside the pipe while h_o is the free convection heat transfer coefficient of air and r_i and r_o are the inner and outer pipe radii. A_i and A_o are the inner and outer heat transfer areas of the radiator and k_p is the pipe thermal conductivity, while L_p refers to the pipe length. Equation (3) can be described in thermal resistance as presented below, see Figure 3.

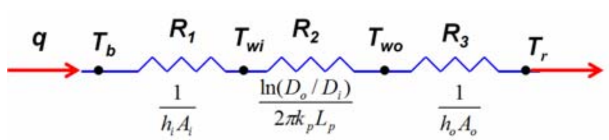

Figure 3. Thermal resistance diagram.

The inner heat transfer coefficient can be obtained by applying equation below:

$$h_i = q/A_i\,(T_b - T_{wi}), \tag{4}$$

where in this study, R_1 is the heat resistance prevailing in between T_b and T_{wi}, R_2 is the heat resistance due to the wall thickness and R_3 is the heat resistance occurring in between outside wall radiator and T_r. $T_b > T_{wi}$, however, T_{wi} is difficult to measure but T_{wo} can be measured directly. Thus, the heat coming out from the radiator wall, q_{fc} (free convection heat transfer rate) can be determined simply as:

$$q_{fc} = \frac{T_{wo} - T_r}{\dfrac{1}{h_o A_o}} = h_o A_o (T_{wo} - T_r). \quad (5)$$

Nevertheless, h_o should be determined and it can be estimated theoretically using correlations proposed by Churchill and Chu [21]:

$$h_o = \frac{k_f}{D_o}\overline{Nu} = \frac{k_f}{D_o}\left\{0.68 + \frac{0.670 Ra^{1/4}}{[1 + (0.492/Pr)^{9/16}]^{4/9}}\right\} \text{ for } Ra < 10^9, \quad (6)$$

h_o is also able to be determined from experiments. When q in equation (1) or (2) is equal to q in equation (5), then h_o can be obtained where T_{wo} and T_r are measured directly. Pr is the Prandtl number, Ra is the Rayleigh number and $\overline{Nu}$ is the average Nusselts number and D_o is the outer diameter of the duct/pipe while k_f is the fluid thermal conductivity. Nevertheless, equation (6) is for vertical planes or pipes (for Case A), while for horizontal pipes (Cases B and C), equation (6) should be replaced by equation (7) which was also proposed by Churchill and Chu [21] and is given by

$$h_o = \frac{k_f}{D_o}\overline{Nu} = \frac{k_f}{D_o}\left\{0.6 + 0.387\left[\frac{Ra}{[1 + (0.559/Pr)^{9/16}]^{16/9}}\right]^{1/6}\right\}^{1/2}$$

$$\text{for } Ra < 10^{12}, \quad (7)$$

Ra is a function of Grashof number $(Ra = GrPr)$:

$$Gr = \frac{g\beta(T_{wo} - T_r)L_p^3}{\nu^2} \text{ for vertical pipes, Case A} \tag{8a}$$

or

$$Gr = \frac{g\beta(T_{wo} - T_r)D_o^3}{\nu^2} \text{ for Case C,} \tag{8b}$$

where β is the expansion coefficient which is equal to $1/T_f$ (T_f is a film temperature). ν is the kinematic viscosity and T_r is the fluid temperature (or air in this study). Then the natural heat transfer coefficient can be usually derived as:

$$h_o = \overline{N}uk_f / D_o. \tag{9}$$

On the other hand, the heat transferring from the fins to the air can be estimated for Case B as:

$$h_{os} = (k_f / S)\left[\frac{576}{(Ra_s S/L)^2} + \frac{2.873}{(Ra_s S/L)^{0.5}}\right]^{-0.5} \tag{10}$$

and

$$Ra_s = PrGr_S = \frac{Prg\beta(T_{wo} - T_r)S^3}{\nu^2}, \tag{11}$$

$$q_s = h_{os} 2nLH(T_{wo} - T_r), \tag{12}$$

where q_s is free convective heat transfer rate from walls and fins to the surrounding, n is the number of the fins, S is the fin spacing, L is the height of the fin and H is the width of the fin. Ra_s refers to the Rayleigh number for fins. Equations (10) to (12) are provided in Cengel [22].

4. Results and Discussion

Heat transfer characteristics presented in this paper are (a) heat transferring from hot water inside the radiator to the radiator wall and (b) heat transferring from the radiator wall to the air inside the prototype room. At the inside of the radiator, the existing heat transfer is due to the hot water flowing in it, while at the outside of the radiator, the prevailing heat transfer is categorized as free convection as the radiator is placed in the calm air inside the prototype room. The heat transfer occurring inside the radiator depends on the mass flow rate and $\Delta T = T_i - T_o$, as well as the specific heat, see equation (1) or (2) or in Holman [19] and Incropera et al. [20]. ΔT for the three cases at the mass flow rate of 12.5g/s is given in Figure 4. ΔT in Figure 4, at the 0 to 1000 seconds fluctuates with big irregular amplitudes. This was caused by the unsteady condition. At the time, the inlet temperature changed from around 30°C to 80°C. The change in the inlet temperature caused the change in the outlet temperature and gave the fluctuation of the outlet temperature. After the inlet temperature reached 80°C and got steady, the ΔT became stable or constant.

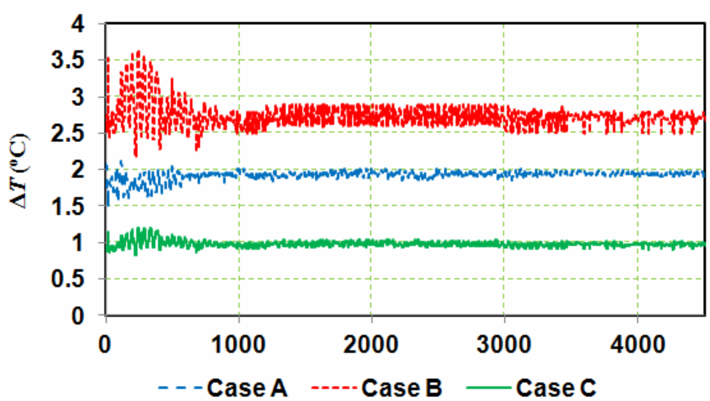

Figure 4. Effect of radiator types on the ΔT at the same water inlet temperature (80°C) and mass flow rate of 12.5g/s.

The highest ΔT was obtained using Case B, while the lowest ΔT was achieved using Case C. The heat transfer rate is strongly affected by the shape/type of the radiator, while effect of mass flow rate on the heat transfer rate was reported by Calisir et al. [13] and Mirmanto et al. [2]. They explained that there was no effect of the mass flow rate on the heat transfer rate at the experimental conditions used. At the mass flow rate of around 12.5g/s, Case B gives the highest ΔT. This is because of the fins. Case B has the biggest heat transfer area. Therefore, Case B results in the higher ΔT value and releases the highest heat rate to the air inside the prototype room. Figure 5 presents the heat transfer rate results calculated using equation (2).

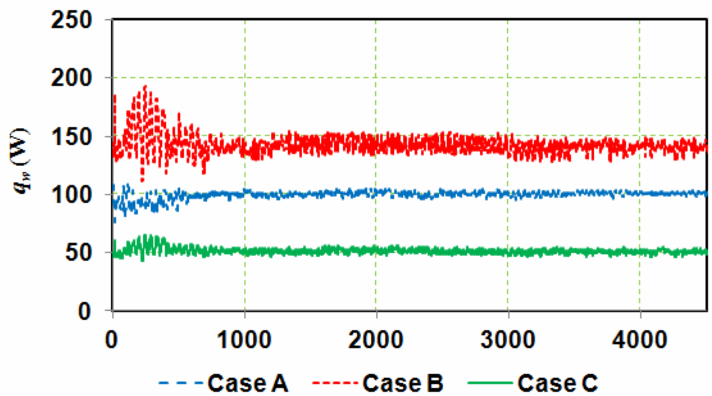

Figure 5. Effect of radiator types on the heat transfer rate at the same water inlet temperature of 80°C and mass flow rate of 12.5g/s.

However, different radiator types show significant differences of the heat transfer rate. Case B results in the highest heat transfer rate of approximately 145W, while Case C gives the lowest heat transfer rate of around 50W. Nevertheless, as mentioned before, the different heat transfer rate is due to the shape/type and the heat transfer area. The bigger heat transfer area gives the higher heat transfer rate. This agrees with the theory, see equation (5). As the heat transfer area for the three radiators is different, it is necessary to present the experimental heat flux, q'', based on the outer heat transfer area to eliminate the effect of the heat transfer area. The heat flux can be calculated as:

$$q'' = q/A_o = \dot{m}c_p(T_i - T_o)/A_o, \tag{13}$$

where A_o is the heat transfer area of the radiator facing to the air inside the prototype room or the outer heat transfer area of the radiator. The area of the radiator can be seen in Table 1 and the experimental heat flux is presented in Figure 6. The highest heat flux value is shown by Case A, while the lowest heat flux is shown by Case B. This phenomenon can logically occur because in the free convection heat transfer, the circulation of the air surrounding the radiator occurs naturally, therefore, the fin may restrict the air circulation especially when the fin spacing is getting narrower or less than 10mm, see [23]. As a result, the air removes less heat from the finned radiator. Hence, in this study, with these experimental conditions, the finned radiator is not the best, but the parallel radiator is. It can be inferred that the finned heat exchanger with a narrow fin gap is good for forced convection but not for free convection.

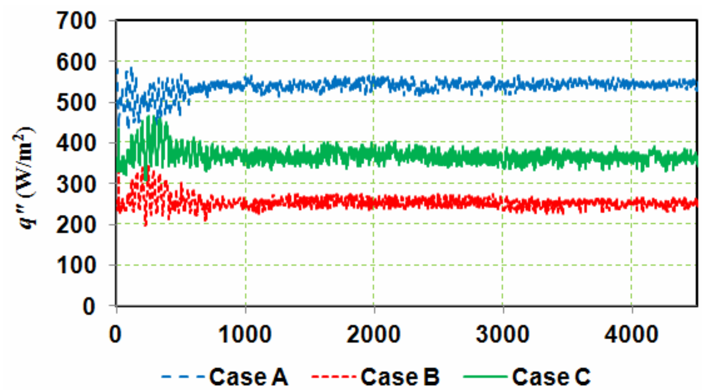

Figure 6. Effect of radiator type on the heat flux based on the outer heat transfer area at the same water inlet temperature of 80°C and mass flow rate of 12.5g/s.

Using the three types of the radiator, the maximum room temperature that could be achieved was approximately 50°C. Different radiator types result in different room temperatures at the same mass flow rate of 12.5g/s. Case B results in the highest room radiator, while Case A and Case C give the lowest room temperature. This again is due to the outer heat transfer area. As presented in Table 1, Case B has the biggest heat transfer area, therefore, it can increase the air temperature from approximately of 30°C to 50°C. The increase of the air temperature inside the prototype room is around 20°C for Case B, while for both Cases A and C is only around 10°C. If the increase in the air temperature is divided by the outer heat transfer area of the radiator to minimize the effect of heat transfer area, then gives $224.8^{\circ}\mathrm{C/m^2}$ for Case A, $89.43^{\circ}\mathrm{C/m^2}$ for Case B and $305.33^{\circ}\mathrm{C/m^2}$ for Case C. From the data, it is difficult to conclude which one is the best because the highest heat flux is achieved using Case A, while the highest temperature flux is achieved using Case C. The highest room temperature was represented by the temperature measured using a thermocouple placed above the radiator of approximately 45cm below the top wall of the prototype room, see Figure 8. The air moved up freely due to the density difference, however, for Cases A and B, the air seemed to be restricted by the body of the radiators as explained in the previous paragraphs. Therefore, the air touched the thermocouple faster for Case C than that for the other radiators. Another reason that can reveal this phenomenon is the height of the radiator. The serpentine radiator has the highest height, it is around 400mm, see Figure 2. Due to the height, the serpentine radiator is closer to the thermocouple, while other radiators are far. Cases A and B have heights of around 300mm and 220mm, respectively. If the height of the serpentine radiator was the same as the other radiators, then the serpentine radiator would give the maximum room temperature of less than 42°C.

The heat released by the water can be cross checked using the heat absorbed by the air inside the prototype room and it shall be the same. The heat released by the water as already discussed above is calculated by applying equation (2), while the heat absorbed by the air can be estimated by utilizing equation (5) for Cases A and C or equation (12) for Case B. Nonetheless, for Case A, to calculate the Grashof number, equation (8a) should be used while for Case C, equation (8b) should be employed. The heat absorbed by the air is presented in Figure 7. The maximum free convection heat transfer rates in this study are approximately 100W for

Case A, 140W for Case B and 50W for Case C. From Figure 7, it can be concluded that the best radiator in this study at these experimental conditions is the parallel radiator (Case A). Therefore, Case A is recommended to be used.

Figure 7. Free convection heat transfer rates absorbed by the air inside the prototype room at the same water inlet temperature (80°C) and mass flow rate of 12.5g/s.

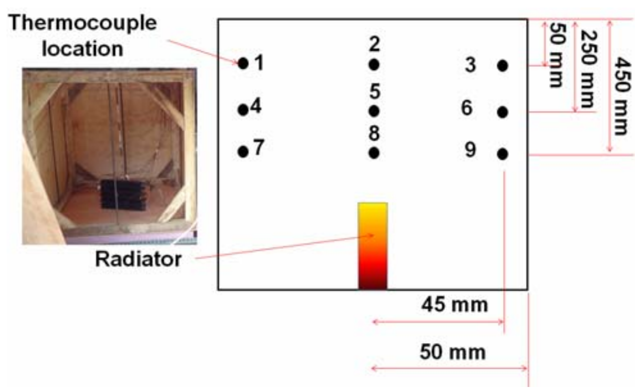

Figure 8. The location of thermocouples inside the prototype room.

There were fifteen thermocouples inserted into the prototype room to measure the room temperature distribution, see Figure 8. As the prototype room is symmetry, then it can be made in a simple view as shown in Figure 8. Using many thermocouples, the air temperature distribution inside the prototype room can be obtained and presented in Figure 9. The locations of the thermocouple were measured from the middle of the room and from the top wall. For example, the thermocouple 8 locates at 0mm (in the middle) and 450mm from the top wall of the room. The thermocouple 6 locates at 45mm (measured from the middle) and 250mm from the top.

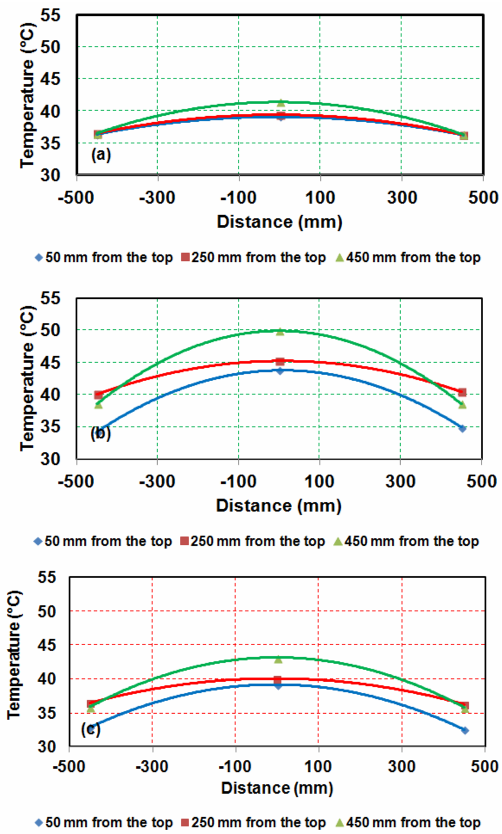

Figure 9. Effect of radiator type on temperature distributions at mass flow rate of 12.5g/s; (a) Case A, (b) Case B and (c) Case C.

Due to the locations or the positions of the thermocouple, each thermocouple gives a different value of a temperature. Thermocouple 8 gives the highest temperature value as it is very close to the radiator and is above the radiator. Therefore, the distribution of the temperature is curvature or parabolic, see Figure 9.

The highest temperature distribution is achieved using the finned radiator as seen in Figure 9. This is, as already mentioned in the previous paragraphs, due to the highest heat transfer area. However, the trend of the temperature distribution for Case B and Case C is almost the same, while for Case A, the temperature distribution is little bit flat. The difference of the temperature at the distances of –450mm, 0mm and 450mm is small for Case A, while for Case B and Case C, the difference is high. The temperature distribution obtained using Case C is higher than that obtained using Case A, however, this is due to the height of the serpentine radiator.

As one of the objectives of this study is to check the free heat transfer coefficient in air site, here the experimental results of the free heat transfer coefficient are presented, see Table 2. From Table 2, it can be seen that the free heat transfer coefficients obtained using Case A are higher than that obtained using Case B and Case C. h_o is calculated using equations (2) and (5). Assuming that all heat transferred from the hot water is the same as the heat absorbed by the air, or as written below:

$$\dot{m}c_p(T_i - T_o) = h_o A_o (T_{wo} - T_r),$$

$$h_o = \frac{\dot{m}c_p(T_i - T_o)}{A_o(T_{wo} - T_r)}, \tag{14}$$

$\dot{m}$, T_i, T_o, T_{wo}, T_r were measured directly. From the results, it is concluded that the parallel radiator is better than others. Case B results in the lower free convection heat transfer because of the heat transfer area.

Table 2. Experimental free heat transfer coefficients

Radiator type or case	Free heat transfer coefficient $(\mathrm{W/m^2K})$
Case A	11.33-13.69
Case B	6.32-7.51
Case C	9.10-11.75

5. Conclusions

An experimental study to investigate the effect of a radiator type on the heat transfer rate and room temperature distribution has been performed and analyzed. From the discussion and results above, some conclusions can be drawn as follows:

(1) The effect of the radiator type on the heat transfer rate is significant.

(2) The maximum heat flux based on the outer heat transfer area is achieved using Case A.

(3) The temperature distribution is curvature.

(4) The experimental heat transfer coefficients agree with the assumption used in the previous published paper for Case B and Case C, while for Case A, it is beyond the assumption.

(5) The best radiator at these experimental conditions is parallel radiator (Case A).

In the future, the energy to heat the water will be obtained from the heat waste or from renewable energy which prevails abundantly and freely in the nature.

Acknowledgement

The authors would like to acknowledge the Indonesia Minister of Research, Technology and Higher Education for the funding with the contract number: No. 61R/SPP-FD/UN18.12/PL/2016, and the Mataram University for the facility.

References

[1] C. R. Coronado, J. T. Yoshioka and J. L. Silveira, Electrical, hot water and cold water production from biomass, Energetic and economical analysis of the compact system of cogeneration run with woodgas from a small downdraft gasifier, J. Renewable Energy 36(6) (2011), 1861-1868.

[2] M. Mirmanto, E. D. Sulistyowati and I. D. K. Okariawan, Effect of radiator position and mass flux on the dryer room heat transfer rate, Results in Physics 6 (2016), 139-144.

[3] J. A. Myhren and S. Holmberg, Performance evaluation of ventilation radiators, Applied Thermal Engineering 51(1-2) (2013), 315-324.

[4] A. Ploskic and S. Holmberg, Performance evaluation of radiant baseboards (skirting) for room heating-an analytical and experimental approach, Applied Thermal Engineering 62(2) (2014), 382-389.

[5] K. Bangert, Radiator heat transfer augmentation by changes to wall surface roughness and emissivity, The University of Sheffield, 2010.

[6] M. Embaye, R. K. Al-Dadah and S. Mahmoud, Effect of flow pulsation on energy consumption of a radiator in a centrally heated building, Int. J. Low-Carbon Technologies (2014), 1-11.

[7] R. Lemlich, Vibration and pulsation boost heat transfer, Chem. Eng. 68 (1961), 171-176.

[8] X. Shuai, S. Cheng and G. Antoni, Pulsation effect on convective heat transfer in the laminar flow of a viscous fluid, J. Chem. Eng. 72 (1994), 468-475.

[9] A. E. Zohir, The influence of pulsation on heat transfer in a heat exchanger for parallel and counter water flows, New York Science Journal 4(6) (2011), 61-71.

[10] I. Liu, L. Fu and Y. Jiang, A new wireless on-off control technique for adjusting and metering household heat in district heating system, Applied Thermal Engineering 36 (2012), 202-209.

[11] B. Lehmanna, D. Gyalistrasb and M. Gwerderc, Intermediate complexity model for model predictive control of integrated room automation, Energy Building 58 (2013), 250-262.

[12] M. Adolph, N. Kopmann and B. Lupulescu, Adaptive control strategies for single room heating, Energy Building 68 (2014), 771-778.

[13] T. Calisir, S. Baskaya, H. O. Yazar and S. Yucedag, Experimental investigation of panel radiator heat output enhancement for efficiency thermal use under actual operating conditions, EPJ Web of Conference 92 (2015).

[14] Mirmanto, D. B. R. Kenning, J. S. Lewis and T. G. Karayiannis, Pressure drop and heat transfer characteristics for single-phase developing flow of water in rectangular microchannels, J. Physics Conference Series 395 (2012), 1-13.

[15] W. Qu and I. Mudawar, Experimental and numerical study of pressure drop and heat transfer in a single-phase micro-channel heat sink, Int. J. Heat and Mass Transfer 45 (2002), 2549-2565.

[16] M. Venkatesan, S. K. Das and A. R. Balakrishnan, Effect of tube diameter on two phase flow patterns in mini tubes, J. Chem. Eng. 88 (2010), 936-944.

[17] M. Mirmanto, Local pressure measurements and heat transfer coefficients of flow boiling in a rectangular microchannel, Heat and Mass Transfer 52(1) (2016), 73-83.

[18] Y. Wang and K. Safiane, Effect of heat flux, vapour quality, channel hydraulic diameter on flow boiling heat transfer in variable aspect ratio microchannels using transparent heating, Int. J. Heat and Mass Transfer 55 (2012), 2235-2243.

[19] J. P. Holman, Heat Transfer, 8th ed., McGraw-Hill Companies, Inc., U.S.A., 1997.

[20] F. P. Incropera, D. P. Dewitt, T. L. Bergman and A. S. Lavine, Fundamental of Heat and Mass Transfer, 6th ed., John Wiley and Sons, U.S.A., 2006.

[21] S. W. Churchill and H. H. S. Chu, Correlating equations for laminar and turbulent free convection from a vertical plate, Int. J. Heat and Mass Transfer 18(11) (1975), 1323-1329.

[22] Y. A. Cengel, Heat Transfer: A Practical Approach, 2nd ed., McGraw-Hill, Mexico, 2004.

[23] http://www.electronics-cooling.com/2002/02/estimating-natural-convection-heat-transfer-for-arrays-of-vertical-parallel-flat-plates/.